Biological Psychiatry: CNNI

Archival Report

Dose-Dependent Target Engagement of a Clinical Intermittent Theta Burst Stimulation Protocol: An Interleaved Transcranial Magnetic Stimulation–Functional Magnetic Resonance Imaging Study in Healthy People

Kai-Yen Chang, Martin Tik, Yuki Mizutani-Tiebel, Paul Taylor, Timo van Hattem, Peter Falkai, Frank Padberg, Lucia Bulubas, and Daniel Keeser

ABSTRACT

BACKGROUND: Intermittent theta burst stimulation (iTBS) of the dorsolateral prefrontal cortex (DLPFC) is widely applied as a therapeutic intervention in mental health; however, the understanding of its mechanisms is still incomplete. Prior magnetic resonance imaging (MRI) studies have mainly used offline iTBS or short sequences in concurrent transcranial magnetic stimulation (TMS)–functional MRI (fMRI). This study investigated a full 600-stimuli iTBS protocol using interleaved TMS-fMRI in comparison with 2 control conditions in healthy subjects.

METHODS: In a crossover design, 18 participants underwent 3 sessions of interleaved iTBS-fMRI: 1) the left DLPFC at 40% resting motor threshold (rMT) intensity, 2) the left DLPFC at 80% rMT intensity, and 3) the left primary motor cortex (M1) at 80% rMT intensity. We compared immediate blood oxygen level–dependent (BOLD) responses during interleaved iTBS-fMRI across these conditions including correlations between individual fMRI BOLD activation and iTBS-induced electric field strength at the target sites.

RESULTS: Whole-brain analysis showed increased activation in several regions following iTBS. Specifically, the left DLPFC, as well as the bilateral M1, anterior cingulate cortex, and insula, showed increased activation during 80% rMT left DLPFC stimulation. Increased BOLD activity in the left DLPFC was observed with neither 40% rMT left DLPFC stimulation nor left M1 80% rMT iTBS, whereas activation in other regions was found to overlap between conditions. Of note, BOLD activation and electric field intensities were only correlated for M1 stimulation and not for the DLPFC conditions.

CONCLUSIONS: This interleaved TMS-fMRI study showed dosage- and target-specific BOLD activation during a 600-stimuli iTBS protocol in healthy individuals. Future studies may use our approach for investigating target engagement in clinical samples.

https://doi.org/10.1016/j.bpsc.2024.08.009

Theta burst stimulation (TBS) is a repetitive transcranial magnetic stimulation (rTMS) protocol and is frequently applied to treat psychiatric disorders due to its shorter duration as compared to standard clinical rTMS protocols. TBS was initially developed by translating burst-patterned stimulation, known to induce long-term potentiation and long-term depression in animal brain slices (1–3), into rTMS protocols in humans to identify protocols that more effectively modulate cortical excitability (4,5). Based on a milestone study by Huang *et al.* (5), 2 main TBS protocols emerged early in the field, i.e., intermittent TBS (iTBS) and continuous TBS, and both protocols originally used 50-Hz rTMS bursts at 5 Hz (theta) frequency with up to 600 total pulses and an intensity of 80% of the active motor threshold (MT). Interestingly, these protocols differ primarily in the intervals for iTBS (i.e., 2 seconds on and 8 seconds off), leading to a facilitation of motor evoked potentials (MEPs) and a reduction of short intracortical inhibition, whereas continuous TBS has the opposite effects. Comprehensive studies in animals and humans suggest that these effects are mediated by the differential interaction of TBS protocols with various neuronal subpopulations including modulation of GABAergic (gamma-aminobutyric acidergic) circuits and glutamatergic neurotransmission (6–12).

Current therapeutic TBS variants are essentially based on the original TBS protocols. For clinical use, these protocols are often extended (e.g., up to 1800 stimuli per session) or are applied as accelerated iTBS with multiple iTBS sessions per day (13). Stimulation intensities have similarly varied across clinical iTBS studies. For instance, major depressive disorder is the most common application of iTBS in psychiatry to date

SEE COMMENTARY ON PAGE 787

© 2024 Society of Biological Psychiatry. Published by Elsevier Inc. This is an open access article under the CC BY license (http://creativecommons.org/licenses/by/4.0/).

(14), with intensities ranging from 80% resting MT (rMT) to 120% rMT across studies (15–19). In contrast to the rapid spread of iTBS in clinical applications, there is comparably scarce preclinical research on specific protocols, their mechanistic understanding is limited, and dose-response relationships need to be established. Moreover, therapeutic effects vary largely among individuals, partially influenced by differences in their structural and functional brain connectivity (20–22).

One method to study the acute effects of rTMS protocols is interleaved (or concurrent) TMS–functional magnetic resonance imaging (TMS-fMRI) in which the blood oxygen level–dependent (BOLD) response is measured during rTMS in an MRI scanner. Most interleaved TMS-fMRI studies have focused on the primary motor cortex (M1) (23–28), while fewer studies investigated its effects on the dorsolateral prefrontal cortex (DLPFC) (29–34). Generally, interleaved TMS-fMRI paradigms have typically used short rTMS bursts or single pulses, rather than full rTMS protocols (27–34). To investigate clinical iTBS protocols in terms of their mechanistic action, we have recently implemented a full 600-stimuli iTBS of the left DLPFC in the interleaved TMS-fMRI approach and have shown its feasibility in healthy individuals and a patient with bipolar depression (35). To extend these findings and to test the dose and target specificity of acute iTBS effects in healthy subjects, we investigated the BOLD effects of 600-stimuli iTBS of the left DLPFC in comparison with a 40% rMT iTBS of the left DLPFC and an 80% rMT intensity iTBS of the M1 region in the interleaved TMS-fMRI paradigm. We expected a maximum BOLD effect in the iTBS target region and connected brain areas. To assess the iTBS neural response in specific regions across subjects, we reported the hemodynamic response function (HRF) beta values to indicate the strength of the BOLD responses to TMS. A larger fMRI-BOLD response, evoked by neural activity, is reflected by a higher beta value estimate. The beta value is widely reported in the concurrent TMS-fMRI field as a method for quantifying the HRF induced by TMS (32,36,37). In addition, we used computational modeling of TMS-induced electric field (E-field) to explore E-field intensity as a further proxy for iTBS dosing (38). In sum, this interleaved TMS-fMRI study investigates first-level hypotheses (i.e., dose and target specificity) on the acute effects of left DLPFC iTBS to establish more specific hypotheses regarding the action of iTBS on brain connectivity, modulation, and function.

METHODS AND MATERIALS

Healthy Participants

The recruitment criteria of healthy adult participants and the detailed procedures are described in the Supplement. A total of 19 healthy participants (8 female, 11 male; ages 21–36 years, average age = 26.4 years, SD = 3.2 years) completed all sessions in this study. One subject was excluded from the group-level analysis due to excessive motion exceeding 3 mm even after motion correction, leaving 18 subjects included in the fMRI analysis. All subjects signed informed consent as approved by the LMU Munich ethical committee prior to participation, and all procedures adhere to the principles outlined in the Declaration of Helsinki.

Experimental Setup

Participants completed 4 experimental sessions, comprising a baseline session without TMS and 3 interleaved iTBS-fMRI sessions. Each subject underwent interleaved iTBS-fMRI sessions with a randomized order of stimulated conditions, including 80% rMT left DLPFC, 40% rMT left DLPFC, and 80% rMT left M1. There was a minimum of 1 week between each session (Figure 1A). The baseline session was performed using a 64-channel standard head coil. In the TMS-fMRI sessions (Figure 1B), we utilized 2 TMS-compatible 7-channel MR coils (39) to cover the whole brain. Neuronavigation (Localite GmbH) was precisely employed to target the predefined anatomical region over the left DLPFC, based on a previous study (16) and individual measured M1 hotspot (Figure 1D). The detailed baseline MRI sequences and neuronavigation setup are described in the Supplement.

Transcranial Magnetic Stimulation. All TMS procedures were conducted inside the MRI scanner room using an MRi-B91 MR-compatible TMS coil and MagProX100 stimulator (MagVenture A/S). A 7-channel surface radiofrequency coil (39) was affixed between the scalp and the MR-compatible TMS coil during MT determination to ensure a matching intensity during interleaved iTBS-fMRI sessions. MT determination was measured exclusively during the baseline session. Participants were lying down with their hands relaxed on the MR scanner bed. An MR-compatible electromyography recorder (Brain Products) was used, with electromyography electrodes placed over the right abductor pollicis brevis, while a ground electrode was positioned over the right ankle. MEPs were identified as responses with amplitudes exceeding 50 μV within 15 to 35 ms following each TMS pulse. The rMT was determined at the optimal coil position for eliciting MEPs in the right abductor pollicis brevis using the standard method (40).

Concurrent TMS-fMRI. The concurrent TMS-fMRI sessions utilized two 7-channel surface radiofrequency coils (39). Structural imaging was performed using a magnetization-prepared 2 rapid acquisition gradient-echo sequence (repetition time = 4000 ms, echo time = 2.98 ms, inversion time 1/inversion time 2 = 700 ms/2500 ms, flip angle 1/flip angle 2 = 4°/5°, 160 slices, 1-mm slice thickness) (41). Interleaved iTBS-fMRI was performed continuously for 3 minutes and 32 seconds (including a 12-second dummy scan) using a multiband accelerated echo-planar imaging sequence (multiband factor of 4, repetition time = 2000 ms, echo time = 30 ms, 40 slices, and voxel size of 3.3 × 3.3 × 3 mm) (Figure 1C).

MRI Data Preprocessing and Statistical Analyses. The detailed preprocessing steps of MRI data are described in the Supplement. Additionally, we used independent component analysis (ICA) to regress out potential coil artifacts caused by eddy/leakage currents or mechanical vibrations in the fMRI data. We applied FSL's MELODIC algorithm (42) to run a single-subject ICA, constraining the output to 15 components. We then manually classified and removed ICs related to noise or artifacts (see Figure S2 for examples of ICA classification). After removing noise ICs, we conducted group analysis using an established block-design analysis pipeline (35).

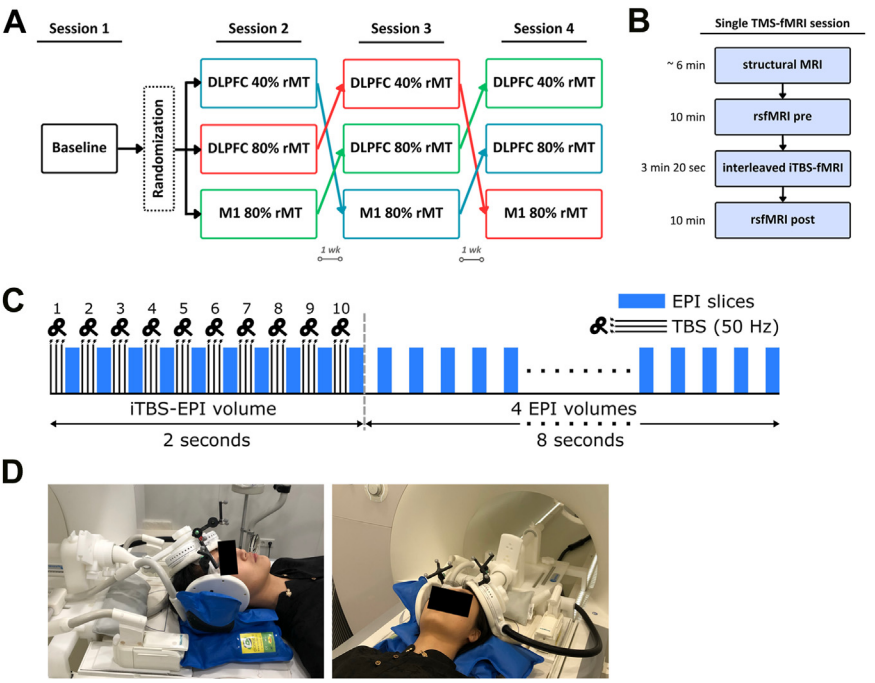


Figure 1. **(A)** The experimental design involved a baseline visit, followed by a randomized 3-way crossover design for interleaved intermittent theta burst stimulation–functional magnetic resonance imaging (iTBS-fMRI) sessions, with a minimum of 1 week washout between each session. **(B)** The MRI scan protocol was consistently used throughout transcranial magnetic stimulation–fMRI (TMS-fMRI) sessions. **(C)** Interleaved iTBS-fMRI sequence, which repeats 20 times, for a total of 3 minutes 20 seconds in the standard iTBS protocol. **(D)** Concurrent TMS-fMRI setup with two 7-channel radiofrequency coils. The MR-compatible TMS coil was mounted on the left radiofrequency coil. The images show (left panel) TMS-MRI coils targeting the left dorsolateral prefrontal cortex (DLPFC) and (right panel) primary motor cortex (M1). EPI, echo-planar imaging; rMT, resting motor threshold; rsfMRI, resting-state fMRI.

Correlation E-Field and BOLD Activation

To test for correlation between the simulated E-field strength and fMRI BOLD activation in each subject in the left DLPFC and left M1, we adopted predefined targets for the left DLPFC (−38, 44, 26 mm Montreal Neurological Institute [MNI]), in which we did the stimulation (16), and M1 (−37, −21, 58 mm MNI) (43). Data from only 16 subjects were included in the DLPFC 80% rMT condition, while 15 subjects were included in the DLPFC 40% rMT and M1 80% rMT conditions due to missing TMS trigger recordings. Subsequently, we calculated the mean E-field magnitude using SimNIBS 4.0 (https://simnibs.github.io/simnibs/build/html/index.html) and the mean HRF beta value from fMRI data within a 10-mm radius of our predefined targets as region of interest. Finally, the correlation coefficient was used to determine the relationship between the E-field magnitude and the fMRI beta value for the M1 and DLPFC conditions.

RESULTS

Immediate BOLD Changes During Interleaved iTBS-fMRI in Healthy Subjects

The 80% rMT iTBS over the left DLPFC represented the main focus of the experiment. The 40% rMT iTBS over the left DLPFC served as a low-intensity control condition, and the 80% rMT iTBS over the left M1 served as an active control condition at a different target region.

Effects of 40% rMT iTBS Over the Left DLPFC. The 40% rMT iTBS-DLPFC (Table 1) did not activate the underlying cortex but instead resulted in BOLD activity in the contralateral, right DLPFC (right superior frontal gyrus, t_{17} = 5.23) (Figure 2A). Similar to the 80% rMT left DLPFC data (see the following), we observed consistent peak BOLD activations in the bilateral auditory cortex (left superior temporal gyrus, t_{17} = 6.68; right superior temporal gyrus, t_{17} = 5.79) and anterior cingulate cortex (ACC) (right ACC, t_{17} = 4.13).

Effects of 80% rMT iTBS Over the Left DLPFC. In the 80% rMT iTBS-DLPFC condition (Table 1), significantly increased BOLD activation was observed locally under the TMS coil in the targeted region, with a focal cluster of BOLD activity localized at the stimulated left DLPFC (left superior frontal gyrus, t_{17}= 5.85) (Figure 2B). The BOLD activation also spread to the bilateral M1 (left precentral gyrus, t_{17} = 4.59; right precentral gyrus, t_{17} = 4.35) and ACC (left ACC, t_{17} = 4.84; right ACC, t_{17} = 4.06). Subcortically, BOLD activation was found in the anterior insula (left anterior insula, t_{17} = 4.66; right anterior insula, t_{17} = 4.72). Furthermore, significant BOLD activity peaks were also observed in the bilateral auditory cortex (left superior temporal gyrus, t_{17} = 6.64; right superior temporal gyrus, t_{17} = 3.85).

Effects of 80% rMT iTBS Over the Left M1. The 80% rMT iTBS-M1 (Table 1) elicited significant BOLD activity in the bilateral M1 (left precentral gyrus, t_{17} = 5.83; right precentral gyrus, t_{17} = 5.7) (Figure 2C), right DLPFC (right middle frontal gyrus, t_{17} = 6.22), right auditory cortex (right superior temporal gyrus, t_{17} = 8), and bilateral primary somatosensory cortex (left postcentral gyrus, t_{17} = 7.3; right postcentral gyrus, t_{17}= 5.83). In the subcortex, BOLD activations were found in the bilateral putamen (right putamen, t_{17} = 5.89; left putamen, t_{17} = 4.76) and left caudate (t_{17} = 4.45).

Table 1. Peak BOLD Activation in Interleaved iTBS-fMRI

Condition	Area	Peak MNI Coordinates, mm[a]	Cluster Size	*t* Value[b]	*z*
40% rMT Left DLPFC	Right superior frontal gyrus	22, 50, 28	354	5.23	3.98
	Right anterior cingulate gyrus	12, 36, 16	127	4.13	3.86
	Left superior temporal gyrus	−58, −12, 14	81	6.68	4.62
	Right superior temporal gyrus	68, −26, 14	72	5.79	4.91
80% rMT Left DLPFC	Left superior frontal gyrus	−22, 60, 24	388	5.85	4.27
	Left precentral gyrus	−60, 10, 28	57	4.59	3.65
	Right precentral gyrus	60, 8, 12	191	4.35	4.75
	Left anterior cingulate gyrus	−2, 30, 16	91	4.84	4.78
	Right anterior cingulate gyrus	4, 32, 16	41	4.06	4.21
	Left anterior insula	−32, 16, −4	45	4.66	3.69
	Right anterior insula	30, 18, 6	60	4.72	3.72
	Left superior temporal gyrus	−64, −18, 8	49	6.64	4.83
	Right superior temporal gyrus	68, −18, 8	40	3.85	4.44
80% rMT Left M1	Right middle frontal gyrus	26, 42, 26	203	6.22	4.43
	Left precentral gyrus	−32, −8, 52	130	5.83	4.26
	Right precentral gyrus	50, 2, 50	164	5.7	4.21
	Right superior temporal gyrus	62, −32, 20	75	8	5.59
	Left postcentral gyrus	−62, −18, 26	81	7.3	4.85
	Right postcentral gyrus	62, −16, 42	71	5.83	4.26
	Left putamen region	−24, 10, 2	44	4.76	3.74
	Right putamen region	26, 14, 2	73	5.89	4.29
	Left caudate region	−10, 4, 14	32	4.45	3.58

The 3 conditions were cluster corrected and thresholded at FWE $p < .05$.

BOLD, blood oxygen level–dependent; DLPFC, dorsolateral prefrontal cortex; fMRI, functional magnetic resonance imaging; FWE, familywise error; iTBS, intermittent theta burst stimulation; M1, primary motor cortex; MNI, Montreal Neurological Institute; rMT, resting motor threshold.

[a]Reported as x, y, z.

[b]$df = 17$.

Correlation of Mean E-Field Magnitude With fMRI in M1 and DLPFC iTBS

This correlation analysis aimed to estimate the relationship between E-field magnitude and fMRI beta values under 3 conditions (Figure 3). No correlation was observed in the 80% rMT or 40% rMT DLPFC condition, with correlation coefficients of $r = 0.30$ ($p = .24$) and $r = -0.14$ ($p = .6$), respectively. Strikingly, in the M1 condition, a strong positive correlation emerged with an $r = 0.65$ ($p = .008$). This suggests that the E-field magnitude was a good indicator of the BOLD response in M1, but no such relationship was observed in the DLPFC.

Individual Variability in Response to Low and High iTBS Intensity Over Bilateral DLPFC

To characterize the iTBS intensity response over the DLPFC in both the stimulated and remote DLPFC regions, and to investigate individual variability due to iTBS, we examined the HRF beta values in each interleaved iTBS-fMRI scan. Remarkably, high-intensity 80% rMT iTBS exhibited a significantly higher beta value in the left DLPFC than low-intensity 40% rMT iTBS ($t_{17} = 2.44$, $p = .03$). Additionally, in the 80% rMT DLPFC condition, the beta value in the left DLPFC was significantly higher than in the right DLPFC ($t_{17} = 2.57$, $p = .02$) (Figure 4B). At the same time, individual variability was apparent (Figure 4C), as some subjects did not demonstrate a strong difference in beta values between high-intensity and low-intensity iTBS. The remote effect of iTBS in the right DLPFC region exhibited considerable individual variability, with no clear evidence that higher intensity leads to a higher beta response in the remote DLPFC region.

DISCUSSION

This interleaved TMS-fMRI study investigated the effects of a full 600-stimuli iTBS protocol at 80% rMT intensity over the left DLPFC in healthy individuals. The iTBS form corresponds to the original iTBS protocol by Huang *et al.* (5), with the only difference that 80% rMT instead of 80% active MT intensity was applied. In the current study, iTBS of the left DLPFC at 80% rMT was compared intraindividually with 40% rMT intensity iTBS to show dose dependency and with 80% rMT M1 iTBS to demonstrate target specificity. We found that 80% rMT DLPFC iTBS led to a BOLD activation within the left DLPFC, with activation extending to a network including the M1 and other connected regions but not the contralateral DLPFC. In contrast, 40% rMT DLPFC iTBS did not show BOLD activation of the underlying cortex but did activate the contralateral prefrontal cortex. M1 iTBS was associated with bilateral BOLD activation in the M1 and extended networks but not in the left DLPFC. Interestingly, BOLD activation of the M1 was correlated with individual E-field strength, whereas this correlation was not observed for the left DLPFC target.

Main Effects of 80% rMT iTBS of the Left DLPFC: Left DLPFC TMS Affects the Left DLPFC

The 80% rMT iTBS left DLPFC condition (Figure 2B) showed BOLD activation of the cortical region at the target site. This

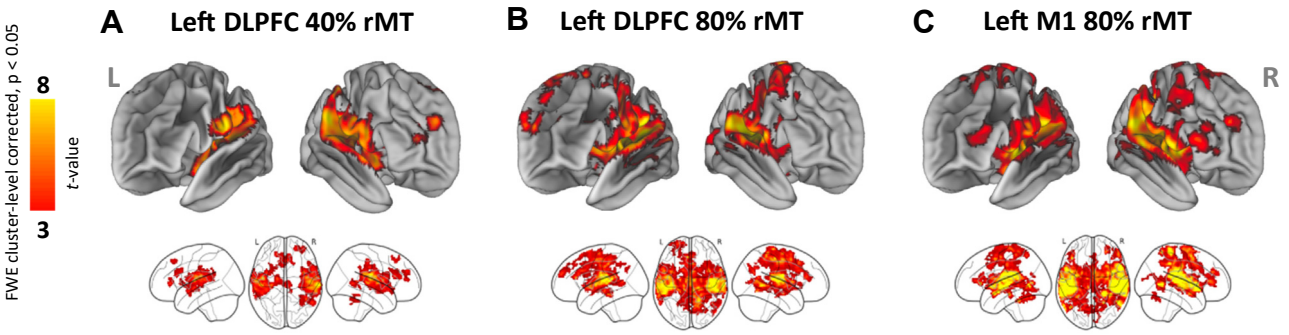


Figure 2. **(A)** Immediate blood oxygen level–dependent (BOLD) changes during 40% resting motor threshold (rMT) left dorsolateral prefrontal cortex (DLPFC) interleaved intermittent theta burst stimulation–functional magnetic resonance imaging (iTBS-fMRI) in healthy subjects. The peak activation in the prefrontal region was found at the right superior frontal gyrus, with $t_{17} = 5.23$. **(B)** Immediate BOLD changes during 80% rMT left DLPFC interleaved iTBS-fMRI in healthy subjects. The peak activation in the prefrontal region was found at the left superior frontal gyrus, with $t_{17} = 5.85$. **(C)** Immediate BOLD changes during 80% rMT left primary motor cortex (M1) interleaved iTBS-fMRI in healthy subjects. The peak BOLD activation was found at the right superior temporal gyrus, with $t_{17} = 8$. FWE, familywise error.

finding aligns with previous concurrent TMS-fMRI studies targeting the DLPFC with various rTMS protocols (31,32). Of note, our data also confirm that TMS not only modulates local neural activity, but also affects distant brain regions, as shown in many prior studies (31,32,36,44,45). We observed increased BOLD signals also in the M1, ACC, anterior insula, and auditory regions. Notably, activation in the ACC and anterior insula is indicative of salience network activity, consistent with Hawco *et al.* (36), who found that targeting the DLPFC with rTMS activates salience nodes, potentially leading to improved treatment outcomes (46). Importantly, while previous studies observed effects through functional connectivity analysis, our study detected effects using a block-design analysis.

Comparison With Low-Intensity and M1 Control Conditions: Target and Dose Specificity

Due to the technical and methodological limitations of iTBS sham conditions (47,48), rather than including a suboptimal sham control condition, our study used 2 well-established active control conditions: 1) low-intensity iTBS at 40% rMT and 2) a second target site, i.e., the M1 region, a target investigated in the majority of previous interleaved TMS-fMRI studies (23,24,26–28,39,49–53).

Applying 40% rMT iTBS to the left DLPFC, we observed fewer voxels showing BOLD activation throughout the brain (Figure 2A). Notably, no significant neural activation was observed at the primary target region, but significant BOLD activation was observed in the contralateral DLPFC. This observation may suggest a potential compensatory mechanism, a phenomenon consistent with findings observed when TMS was applied to other targets and only affected distal sites (51,54). BOLD activation of ACC and auditory regions was weaker than that observed with 80% rMT stimulation, which could be explained by reduced levels of noise and pain during iTBS at 40% intensity. This aligns with our subjects' pain ratings during interleaved iTBS-fMRI (Figure S1); 80% rMT iTBS-DLPFC induced significantly greater pain compared with the

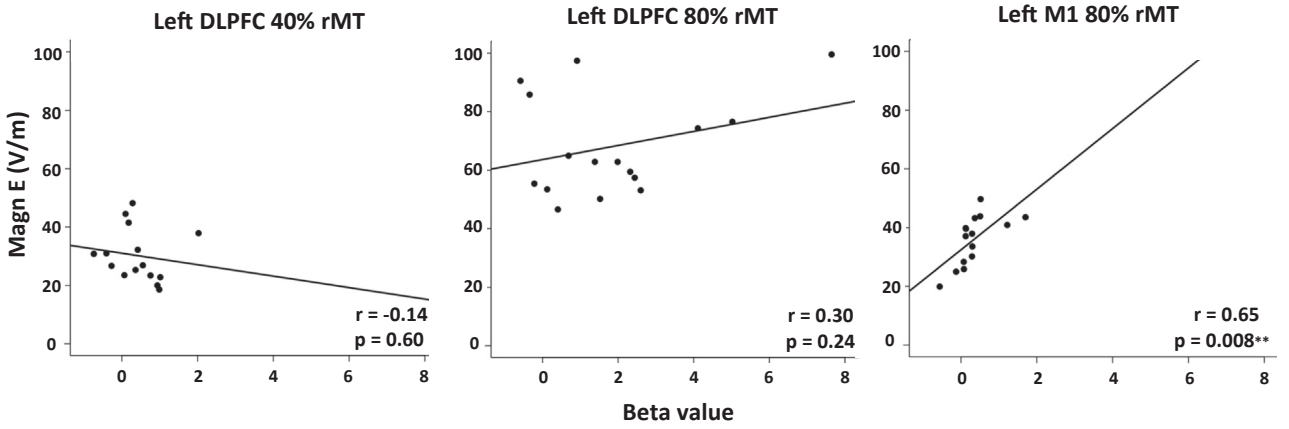


Figure 3. Correlation analysis of electric field magnitude (Magn E) and functional magnetic resonance imaging beta values in 40% resting motor threshold (rMT) dorsolateral prefrontal cortex (DLPFC), 80% rMT DLPFC, and 80% rMT primary motor cortex (M1) conditions. The 40% rMT DLPFC condition showed no correlation, with $r = -0.14$ ($p = .6$), and neither did the 80% rMT DLPFC condition, with $r = 0.3$ ($p = .24$), while in the M1 condition, a strong positive correlation was observed, with $r = 0.65$ ($p = .008$). $^{**}p < .01$.

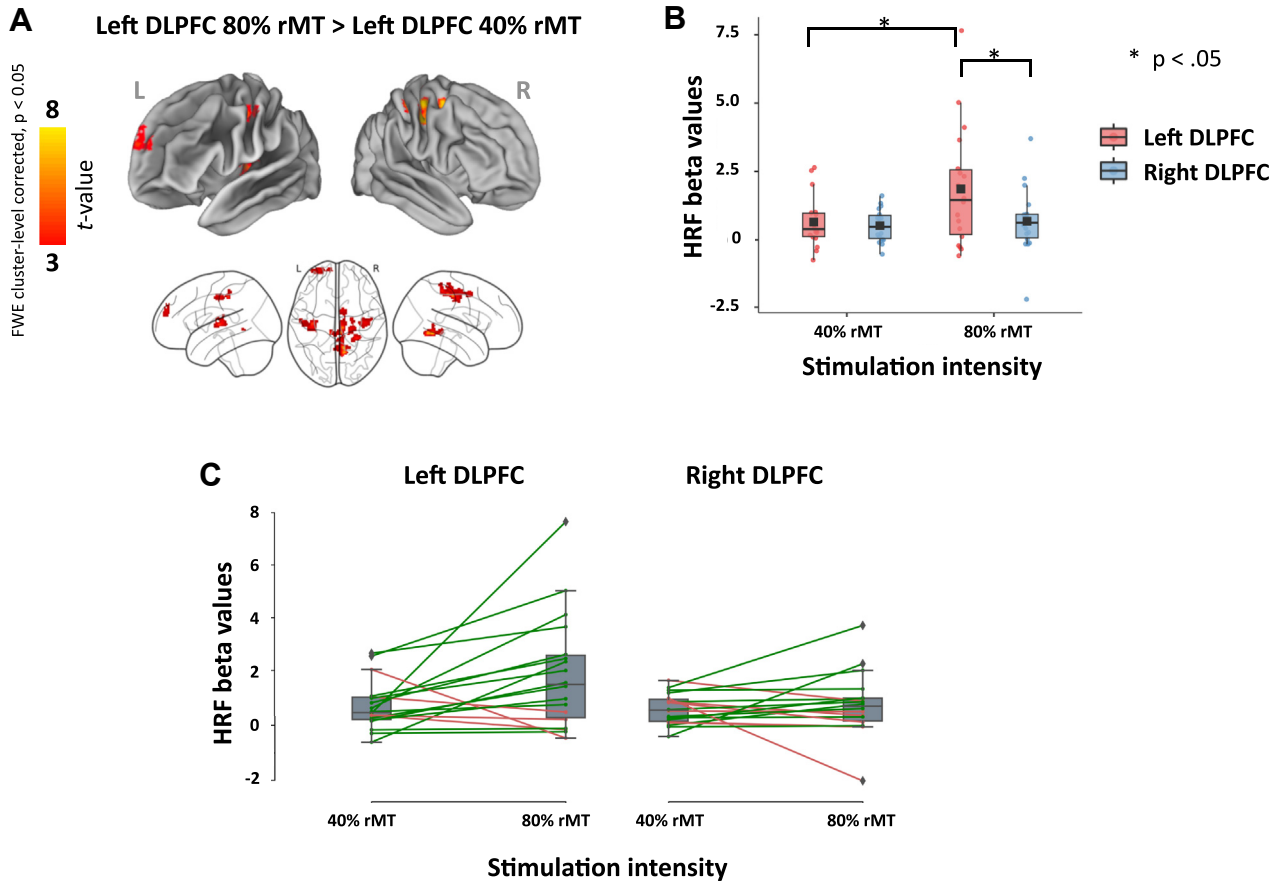


Figure 4. **(A)** For 80% resting motor threshold (rMT) stimulation intensity, there was a stronger activation in the left (L) dorsolateral prefrontal cortex (DLPFC) and a slightly stronger activation in auditory regions compared to 40% rMT stimulation intensity. **(B)** Average hemodynamic response function (HRF) beta values in the left and right (R) DLPFC regions of interest, demonstrating significant differences between low and high stimulation intensities in the left DLPFC. **(C)** Individual variability of HRF beta values for 40% and 80% rMT stimulation intensity over the left and right DLPFC regions of interest, respectively. The green lines indicate individuals who showed a stronger activation with 80% rMT intensity, while the red lines indicate individuals who showed a stronger activation with 40% rMT intensity. FWE, familywise error.

other two conditions. Recent findings in a sham condition by Tik *et al.* (31) showed intensity-dependent effects on somatosensory and auditory cortex regions but no effects on the ACC. Overall, our findings support the hypotheses that decreasing the strength of stimulation results in changes in remote areas as well (36,55,56). While demonstrating dose-dependent effects of iTBS, there is no established lower threshold for neurophysiological effects of iTBS. Thus, iTBS protocols with intensities below 80% rMT may depolarize subpopulations of interneurons and modulate cortex excitability (9).

As a second control condition, we included 80% rMT iTBS-M1 to identify regions that are activated by iTBS of the left DLPFC but not activated by 80% rMT iTBS of M1. As expected, we observed activation in the bilateral M1 and somatosensory cortex regions during iTBS-M1, consistent with previous research (57,58). However, we observed that the iTBS-M1 neural activity extended widely to the right DLPFC, contradicting a prior study that suggested that the effects of iTBS-M1 do not spread rostrally to the PFC (37). Nonetheless, our results align with previous findings indicating that M1 TMS can indeed propagate through anatomical projections to affect more distant regions such as the putamen (37,44,57).

Dose-Dependent Target Engagement and Interindividual Variability of E-Field With fMRI

To compare the interindividual dose-response relationship between M1 and DLPFC iTBS, MR-based E-field modeling was applied for both target sites and tested for a correlation with the fMRI beta value during iTBS. Only for the M1 was a significant positive correlation between fMRI BOLD activation and E-field magnitude found across subjects, while we did not observe such a correlation in the DLPFC conditions at either intensity. This finding was even more surprising because iTBS intensities are already personalized to the individual rMT. The most likely explanation for the difference between the M1 and left DLPFC targets in this respect is that the M1 target is functionally established (i.e., as a hotspot with the largest MEP amplitudes for the contralateral abductor pollicis brevis muscle), whereas the TMS coil position over the left DLPFC

followed anatomical landmarks (i.e., predefined MNI target). Thus, both factors, i.e., more variable positioning in relation to individual cortical structures and higher variability of functional connectivity in prefrontal as compared with motor networks (59), may contribute to the larger variation of BOLD activation in relation to E-field intensities for the 80% rMT iTBS-DLPFC condition. To reduce this variance in DLPFC targeting procedures, it is crucial to identify common biomarkers for rTMS therapeutic protocols and optimize personalized DLPFC targeting for clinical treatment. Several studies have shown that using fMRI to localize the DLPFC target region based on its anticorrelation with the subgenual ACC may represent an individualized target site for rTMS, resulting in improved psychiatric treatment outcomes (60–62). In addition, previous research has highlighted the variation in brain area depths (63), which our data also indicate with differences in coil-to-cortex distance between the DLPFC and M1 (see Figure S7). This underscores the importance of employing E-field modeling to adjust the TMS intensity across different brain regions, thereby ensuring stimulation of brain areas with equivalent effective strength as estimated for the M1 (38,64,65).

Furthermore, our findings suggest a dose-response relationship in the left DLPFC between 40% rMT and 80% rMT iTBS, in which higher stimulation intensity correlates with higher beta values. However, this pattern was not found for distant effects in the right DLPFC. In addition, we observed interindividual variability for the left DLPFC effect, with activation patterns differing among subjects at both 80% rMT and 40% rMT TMS intensities. For instance, not all subjects demonstrated consistently higher beta values with increased TMS intensity (Figure 4C). Such variability may offer insights into the varied responses to prefrontal TMS, but the current sample was too small for further analyzing this variability to reach meaningful conclusions.

Current and Previous Findings With Interleaved TMS-fMRI

In the study, 3 conditions featuring different stimulation locations and intensities showed widespread BOLD activation across multiple brain regions. This concurs with previous interleaved TMS-fMRI studies, with single pulses of TMS over the DLPFC leading to changes in BOLD signal across multiple brain areas, including the stimulated target and its contralateral region, subcortical regions, and auditory cortex (66,67). Furthermore, previous interleaved TMS-fMRI studies have also demonstrated a dose-response relationship between stimulation intensity and BOLD signals for M1 and DLPFC targets (26,32,44,51), aligning with our findings.

In addition, we assessed the feasibility of an ICA denoising strategy and compared it with our previous study without ICA denoising (35). Our observations revealed that 80% rMT iTBS-DLPFC had less extensive BOLD activation in stimulated and remote regions after implementing ICA denoising. ICA denoising has also been recommended as an essential step in concurrent TMS-fMRI (37). Various potential MRI artifacts can arise during data acquisition due to interactions with concurrent TMS. These artifacts may be attributed to factors such as magnetic susceptibility, vibration, thermal drift, leakage current originating from the TMS coil, coupling effects between the TMS device and the MRI hardware, and the echo-planar imaging sequence (27,28,68). These effects can be apparent as a reduced signal-to-noise ratio under the TMS coil. In some cases, image artifacts can occur, affecting data quality for durations ranging from milliseconds to minutes, and in extreme cases, even permanently (37). Here, we highlight a significant concern within the concurrent TMS-fMRI field that the potential data analysis method may induce a high type II error (false negatives), primarily attributable to factors such as motion artifacts or interaction between TMS and fMRI acquisition.

Limitations

We are aware that the current study has limitations: First, our findings may not be generalizable to other iTBS protocols, e.g., the Food and Drug Administration–cleared protocol for major depressive disorder, in which 120% rMT intensity (16) or longer iTBS sessions with 1800 stimuli were used. Second, the sample is small, and the study has limited power for conducting further secondary analyses. Thus, we may regard many of our findings as preliminary and hypothesis-generating. Third, it would be extremely challenging to disentangle direct neural activation by iTBS versus activation by sensory stimulation (e.g., noise from TMS and MRI or somatosensory artifacts and pain), novelty experience, or expectation, which might result, e.g., in large-scale activation observed in the ACC, putamen, and insula. Fourth, other potential sources of interindividual variability in our results may arise from biological differences between our healthy participants, such as gender, age, and brain state and structure, and furthermore, technical variability during the TMS-fMRI setup, e.g., TMS targeting, coil-to-cortex distance, and artificial induction between TMS and MRI. Additionally, heterogeneity in brain anatomy might be relevant as well, as indicated by interindividual differences in the coil-to-cortex distance (see Figure S7). At the analysis level, the inclusion of ICA denoising may introduce bias in removing ICs, potentially leading to variability in the sources detected. However, we still emphasize the importance of establishing an appropriate fMRI data preprocessing and analysis pipeline for future concurrent TMS-fMRI studies. Our study underscores the distinctive challenges presented by concurrent TMS-fMRI, e.g., the use of low-channel birdcage or thin-film surface coils during concurrent TMS-fMRI imaging sessions can lead to inferior MR image quality and incomplete coverage of the brain. Moreover, the interaction between TMS pulses and the MRI coil, particularly the high magnetic field and current leakage from TMS coil, can cause image distortion in milliseconds to seconds. This requires thorough attention to configuring concurrent TMS-fMRI sequences and during both pre- and postprocessing stages of data analysis.

Future Directions and Perspectives

The common challenges encountered in concurrent TMS-fMRI studies, including target engagement, complex setups, technical constraints, and the absence of an optimal sham condition, are also applicable to our study, as highlighted previously (28,35). At all levels, there is space for refining current interleaved TMS-fMRI methodology. The findings of the current study may therefore guide future development of experimental TMS-fMRI setups to investigate clinical iTBS protocols in

transdiagnostic samples and healthy subjects, with the overarching goal to better understand effects and mechanisms of therapeutic iTBS in relation to the individual brain connectivity and function. Concurrent TMS-fMRI represents a promising research area, as it holds the potential to identify biomarkers for therapeutic rTMS protocols and to leverage personalized treatment approaches.

Conclusions

This interleaved TMS-fMRI study revealed acute BOLD activation in DLPFC and M1 regions during a 600-stimuli iTBS session in healthy subjects, which was target and dose specific. Compared with iTBS over the M1, in which BOLD activation and iTBS E-field intensity were correlated, high interindividual variability was observed in this respect for iTBS of the left DLPFC. In addition, large-scale BOLD effects were found across all iTBS conditions, which not only may be due to nonspecific activation within the complex experimental setup, but also may be partially due to remote effects of the iTBS protocol. However, the differential impact of these factors cannot be further disentangled with the current study design. Our findings provide guidance for future studies to develop the TMS-fMRI approach toward a paradigm that enables mechanistic research on therapeutic rTMS protocols and a deeper understanding of the rTMS-brain interplay.

ACKNOWLEDGMENTS AND DISCLOSURES

This project was funded by the Federal Ministry of Education and Research within the ERA-NET NEURON program (Grant No. FKZ: 01EW1903: DisCoVeR) and the German Center for Mental Health (Grant No. 01EE2303, project MUC6). The procurement of the Prisma 3T MRI scanner was supported by the Deutsche Forschungsgemeinschaft (Grant No. INST 86/1739-1 FUGG). LB's work was part of the funding program of the Medical Faculty of LMU (FöFöLe Plus, Munich Clinician Scientist Program). MT's travel costs and research stays were supported by the visiting scholarship artificial intelligence programme (BaCaTeC 2022/01, Machine learning-based optimization for personalized brain stimulation therapy). PT's work was funded by the Deutsche Forschungsgemeinschaft (Grant No. TA 857/3-2).

K-YC: conceptualization, formal analysis, investigation, methodology, project administration, visualization, writing – original draft. MT: conceptualization, methodology, supervision, validation. YM-T: conceptualization, investigation, methodology, project administration. PT: writing – review & editing. TvH: visualization, writing – review & editing. PF: funding acquisition, supervision. FP: conceptualization, funding acquisition, methodology, project administration, resources, supervision, validation, writing – review & editing. LB: conceptualization, funding acquisition, methodology, project administration, resources, supervision, writing – review & editing. DK: conceptualization, formal analysis, funding acquisition, methodology, project administration, resources, supervision, validation, visualization, writing – review & editing.

We thank Linda Schuster, Zane Wilkinson, and Cuici Voon for assisting TMS-fMRI data collection and Larissa Behnke for E-field simulation data preprocessing. We thank Christian Windischberger (Center for Medical Physics and Biomedical Engineering at the Medical University of Vienna, Austria) for providing his comprehensive expertise in concurrent TMS-MRI, as well as Patrik Kunz (Localite GmbH, Bonn, Germany) and Matthias Kienle (MagVenture A/S, Farum, Denmark) for their kind support with the technical setup.

Access to the completed MRI data is available upon request. The data can be obtained upon formalizing a data sharing agreement, though not publicly accessible due to challenges in achieving complete anonymization. Unthresholded statistical maps of MRI data are provided on NeuroSynth.

This work is a part of K-YC's Ph.D. program at Munich Medical Research School. YM-T received remuneration from neuroCare Group AG as a part-time office worker. FP is a member of the European Scientific Advisory Board of BrainsWay Inc. (Jerusalem, Israel), and the International Scientific Advisory Board of Sooma (Helsinki, Finland); he has received speaker honoraria from Mag&More GmbH, the neuroCare Group (Munich, Germany), and BrainsWay Inc.; his lab has received support with equipment from neuroConn GmbH (Ilmenau, Germany), Mag&More GmbH, and BrainsWay Inc. PF has received grants and served as consultant, advisor, or continuing medical education speaker for Abbott, GlaxoSmithKline, Janssen, Essex, Lundbeck, Otsuka, Gedeon Richter, Servier, Takeda, the German Ministry of Science, and the German Ministry of Health. All other authors report no biomedical financial interests or potential conflicts of interest.

ARTICLE INFORMATION

From the Department of Psychiatry and Psychotherapy, LMU University Hospital, LMU Munich, Munich, Germany (K-YC, YM-T, TvH, PF, FP, LB, DK); Neuroimaging Core Unit Munich, LMU University Hospital, LMU Munich, Munich, Germany (K-YC, YM-T, TvH, PF, FP, LB, DK); German Center for Mental Health, Partner Site Munich-Augsburg, Germany (K-YC, YM-T, TvH, PF, FP, LB, DK); High Field MR Center, Center for Medical Physics and Biomedical Engineering, Medical University of Vienna, Vienna, Austria (MT); Brain Stimulation Lab, Department of Psychiatry and Behavioral Sciences, Stanford University, Stanford, California (MT); and Department of Psychology, LMU Munich, Munich, Germany (PT).

LB and DK contributed equally to this work.

Address correspondence to Frank Padberg, M.D., at frank.padberg@med.uni-muenchen.de.

Received Apr 29, 2024; revised Aug 8, 2024; accepted Aug 12, 2024.

Supplementary material cited in this article is available online at https://doi.org/10.1016/j.bpsc.2024.08.009.

REFERENCES

1. Larson J, Lynch G (1986): Induction of synaptic potentiation in hippocampus by patterned stimulation involves two events. Science 232:985–988.
2. Larson J, Lynch G (1989): Theta pattern stimulation and the induction of LTP: The sequence in which synapses are stimulated determines the degree to which they potentiate. Brain Res 489:49–58.
3. Capocchi G, Zampolini M, Larson J (1992): Theta burst stimulation is optimal for induction of LTP at both apical and basal dendritic synapses on hippocampal CA1 neurons. Brain Res 591:332–336.
4. Huang YZ, Rothwell JC (2004): The effect of short-duration bursts of high-frequency, low-intensity transcranial magnetic stimulation on the human motor cortex. Clin Neurophysiol 115:1069–1075.
5. Huang YZ, Edwards MJ, Rounis E, Bhatia KP, Rothwell JC (2005): Theta burst stimulation of the human motor cortex. Neuron 45: 201–206.
6. Huang YZ, Chen RS, Rothwell JC, Wen HY (2007): The after-effect of human theta burst stimulation is NMDA receptor dependent. Clin Neurophysiol 118:1028–1032.
7. Ishikawa S, Matsunaga K, Nakanishi R, Kawahira K, Murayama N, Tsuji S, *et al.* (2007): Effect of theta burst stimulation over the human sensorimotor cortex on motor and somatosensory evoked potentials. Clin Neurophysiol 118:1033–1043.
8. Labedi A, Benali A, Mix A, Neubacher U, Funke K (2014): Modulation of inhibitory activity markers by intermittent theta-burst stimulation in rat cortex is NMDA-receptor dependent. Brain Stimul 7:394–400.
9. Suppa A, Huang YZ, Funke K, Ridding MC, Cheeran B, Di Lazzaro V, *et al.* (2016): Ten years of theta burst stimulation in humans: Established knowledge, unknowns and prospects. Brain Stimul 9:323–335.
10. Schilberg L, Schuhmann T, Sack AT (2017): Interindividual variability and intraindividual reliability of intermittent theta burst stimulation-induced neuroplasticity mechanisms in the healthy brain. J Cogn Neurosci 29:1022–1032.
11. Li C, Huang Y, Bai Y, Tsai S, Su T, Cheng C (2019): Critical role of glutamatergic and GABAergic neurotransmission in the central mechanisms of theta-burst stimulation. Hum Brain Mapp 40:2001–2009.

12. Rounis E, Huang YZ (2020): Theta burst stimulation in humans: A need for better understanding effects of brain stimulation in health and disease. Exp Brain Res 238:1707–1714.
13. Neuteboom D, Zantvoord JB, Goya-Maldonado R, Wilkening J, Dols A, Van Exel E, *et al.* (2023): Accelerated intermittent theta burst stimulation in major depressive disorder: A systematic review. Psychiatry Res 327:115429.
14. Haiyang C, Liuqing S, Mei L, Chuntong Z, Mingjie L, Junjing M, *et al.* (2025): Reflections on "Theta burst stimulation for depression: A systematic review and network and pairwise meta-analysis." Mol Psychiatry 30:351–352.
15. Holzer M, Padberg F (2010): Intermittent theta burst stimulation (iTBS) ameliorates therapy-resistant depression: A case series. Brain Stimul 3:181–183.
16. Blumberger DM, Vila-Rodriguez F, Thorpe KE, Feffer K, Noda Y, Giacobbe P, *et al.* (2018): Effectiveness of theta burst versus high-frequency repetitive transcranial magnetic stimulation in patients with depression (THREE-D): A randomised non-inferiority trial. Lancet 391:1683–1692.
17. Chen L, Thomas EHX, Kaewpijit P, Miljevic A, Hughes R, Hahn L, *et al.* (2021): Accelerated theta burst stimulation for the treatment of depression: A randomised controlled trial. Brain Stimul 14:1095–1105.
18. Bulteau S, Laurin A, Pere M, Fayet G, Thomas-Ollivier V, Deschamps T, *et al.* (2022): Intermittent theta burst stimulation (iTBS) versus 10 Hz high-frequency repetitive transcranial magnetic stimulation (rTMS) to alleviate treatment-resistant unipolar depression: A randomized controlled trial (THETA-DEP). Brain Stimul 15:870–880.
19. Morriss R, Briley PM, Webster L, Abdelghani M, Barber S, Bates P, *et al.* (2024): Connectivity-guided intermittent theta burst versus repetitive transcranial magnetic stimulation for treatment-resistant depression: A randomized controlled trial. Nat Med 30:403–413.
20. Cash RFH, Cocchi L, Lv J, Wu Y, Fitzgerald PB, Zalesky A (2021): Personalized connectivity-guided DLPFC-TMS for depression: Advancing computational feasibility, precision and reproducibility. Hum Brain Mapp 42:4155–4172.
21. Elbau IG, Lynch CJ, Downar J, Vila-Rodriguez F, Power JD, Solomonov N, *et al.* (2023): Functional connectivity mapping for rTMS target selection in depression. Am J Psychiatry 180:230–240.
22. Cash RFH, Zalesky A (2024): Personalized and circuit-based transcranial magnetic stimulation: Evidence, controversies, and opportunities. Biol Psychiatry 95:510–522.
23. Bohning DE, Shastri A, McConnell K, Nahas Z, Lorberbaum J, Roberts D, *et al.* (1999): A combined TMS/fMRI study of intensity-dependent TMS over motor cortex. Biol Psychiatry 45:385–394.
24. Hanakawa T, Mima T, Matsumoto R, Abe M, Inouchi M, Urayama S i, *et al.* (2009): Stimulus-response profile during single-pulse transcranial magnetic stimulation to the primary motor cortex. Cereb Cortex 19:2605–2615.
25. Shitara H, Shinozaki T, Takagishi K, Honda M, Hanakawa T (2013): Movement and afferent representations in human motor areas: A simultaneous neuroimaging and transcranial magnetic/peripheral nerve-stimulation study. Front Hum Neurosci 7:554.
26. Navarro de Lara LI, Tik M, Woletz M, Frass-Kriegl R, Moser E, Laistler E, *et al.* (2017): High-sensitivity TMS/fMRI of the human motor cortex using a dedicated multichannel MR coil. NeuroImage 150:262–269.
27. Bergmann TO, Varatheeswaran R, Hanlon CA, Madsen KH, Thielscher A, Siebner HR (2021): Concurrent TMS-fMRI for causal network perturbation and proof of target engagement. NeuroImage 237:118093.
28. Mizutani-Tiebel Y, Tik M, Chang KY, Padberg F, Soldini A, Wilkinson Z, *et al.* (2022): Concurrent TMS-fMRI: Technical challenges, developments, and overview of previous studies. Front Psychiatry 13:825205.
29. Hawco C, Armony JL, Daskalakis ZJ, Berlim MT, Chakravarty MM, Pike GB, *et al.* (2017): Differing time of onset of concurrent TMS-fMRI during associative memory encoding: A measure of dynamic connectivity. Front Hum Neurosci 11:404.
30. Webler RD, Hamady C, Molnar C, Johnson K, Bonilha L, Anderson BS, *et al.* (2020): Decreased interhemispheric connectivity and increased cortical excitability in unmedicated schizophrenia: A prefrontal interleaved TMS fMRI study. Brain Stimul 13:1467–1475.
31. Tik M, Woletz M, Schuler AL, Vasileiadi M, Cash RFH, Zalesky A, *et al.* (2023): Acute TMS/fMRI response explains offline TMS network effects – An interleaved TMS-fMRI study. NeuroImage 267:119833.
32. Tik M, Vasileiadi M, Woletz M, Linhardt D, Schuler AL, Williams N, *et al.* (2023): Concurrent TMS/fMRI reveals individual DLPFC dose-response pattern. NeuroImage 282:120394.
33. Ge R, Humaira A, Gregory E, Alamian G, MacMillan EL, Barlow L, *et al.* (2022): Predictive value of acute neuroplastic response to rTMS in treatment outcome in depression: A concurrent TMS-fMRI trial. Am J Psychiatry 179:500–508.
34. Grosshagauer S, Woletz M, Vasileiadi M, Linhardt D, Nohava L, Schuler A-L, *et al.* (2024): Chronometric TMS-fMRI of personalized left dorsolateral prefrontal target reveals state-dependency of subgenual anterior cingulate cortex effects. Mol Psychiatry 29:2678–2688.
35. Chang KY, Tik M, Mizutani-Tiebel Y, Schuler AL, Taylor P, Campana M, *et al.* (2024): Neural response during prefrontal theta burst stimulation: Interleaved TMS-fMRI of full iTBS protocols. NeuroImage 291:120596.
36. Hawco C, Voineskos AN, Steeves JKE, Dickie EW, Viviano JD, Downar J, *et al.* (2018): Spread of activity following TMS is related to intrinsic resting connectivity to the salience network: A concurrent TMS-fMRI study. Cortex 108:160–172.
37. Riddle J, Scimeca JM, Pagnotta MF, Inglis B, Sheltraw D, Muse-Fisher C, *et al.* (2022): A guide for concurrent TMS-fMRI to investigate functional brain networks. Front Hum Neurosci 16:1050605.
38. Dannhauer M, Gomez LJ, Robins PL, Wang D, Hasan NI, Thielscher A, *et al.* (2024): Electric field modeling in personalizing transcranial magnetic stimulation interventions. Biol Psychiatry 95:494–501.
39. Navarro de Lara LI, Windischberger C, Kuehne A, Woletz M, Sieg J, Bestmann S, *et al.* (2015): A novel coil array for combined TMS/fMRI experiments at 3 T. Magn Reson Med 74:1492–1501.
40. Rossini PM, Burke D, Chen R, Cohen LG, Daskalakis Z, Di Iorio R, *et al.* (2015): Non-invasive electrical and magnetic stimulation of the brain, spinal cord, roots and peripheral nerves: Basic principles and procedures for routine clinical and research application. An updated report from an I.F.C.N. Committee. Clin Neurophysiol 126:1071–1107.
41. Marques JP, Kober T, Krueger G, van der Zwaag W, Van de Moortele PF, Gruetter R (2010): MP2RAGE, a self bias-field corrected sequence for improved segmentation and T1-mapping at high field. NeuroImage 49:1271–1281.
42. Jenkinson M, Beckmann CF, Behrens TEJ, Woolrich MW, Smith SM (2012): FSL. NeuroImage 62:782–790.
43. Mayka MA, Corcos DM, Leurgans SE, Vaillancourt DE (2006): Three-dimensional locations and boundaries of motor and premotor cortices as defined by functional brain imaging: A meta-analysis. NeuroImage 31:1453–1474.
44. Bestmann S, Baudewig J, Siebner HR, Rothwell JC, Frahm J (2004): Functional MRI of the immediate impact of transcranial magnetic stimulation on cortical and subcortical motor circuits. Eur J Neurosci 19:1950–1962.
45. Beynel L, Powers JP, Appelbaum LG (2020): Effects of repetitive transcranial magnetic stimulation on resting-state connectivity: A systematic review. NeuroImage 211:116596.
46. Downar J, Blumberger DM, Daskalakis ZJ (2016): The neural crossroads of psychiatric illness: An emerging target for brain stimulation. Trends Cogn Sci 20:107–120.
47. Duecker F, Sack AT (2015): Rethinking the role of sham TMS. Front Psychol 6:210.
48. Bagali K, Sreeraj VS, Mehta UM, Venkatasubramanian G, Thirthalli J (2023): Feasibility of intermediate theta burst stimulation as sham control in therapeutic transcranial magnetic stimulation studies. Asian J Psychiatry 79:103390.
49. Bohning DE, Shastri A, Nahas Z, Lorberbaum JP, Andersen SW, Dannels WR, *et al.* (1998): Echoplanar BOLD fMRI of brain activation induced by concurrent transcranial magnetic stimulation. Invest Radiol 33:336–340.
50. Baudewig J, Siebner HR, Bestmann S, Tergau F, Tings T, Paulus W, *et al.* (2001): Functional MRI of cortical activations induced by transcranial magnetic stimulation (TMS). Neuroreport 12:3543–3548.

51. Bestmann S, Baudewig J, Siebner HR, Rothwell JC, Frahm J (2003): Subthreshold high-frequency TMS of human primary motor cortex modulates interconnected frontal motor areas as detected by interleaved fMRI-TMS. NeuroImage 20:1685–1696.
52. Denslow S, Lomarev M, George MS, Bohning DE (2005): Cortical and subcortical brain effects of transcranial magnetic stimulation (TMS)-induced movement: An interleaved TMS/functional magnetic resonance imaging study. Biol Psychiatry 57:752–760.
53. Shitara H, Shinozaki T, Takagishi K, Honda M, Hanakawa T (2011): Time course and spatial distribution of fMRI signal changes during single-pulse transcranial magnetic stimulation to the primary motor cortex. NeuroImage 56:1469–1479.
54. Lee TG, D'Esposito M (2012): The dynamic nature of top-down signals originating from prefrontal cortex: A combined fMRI–TMS study. J Neurosci 32(44):15458–15466.
55. Nahas Z, Lomarev M, Roberts DR, Shastri A, Lorberbaum JP, Teneback C, *et al.* (2001): Unilateral left prefrontal transcranial magnetic stimulation (TMS) produces intensity-dependent bilateral effects as measured by interleaved BOLD fMRI. Biol Psychiatry 50:712–720.
56. Nettekoven C, Volz LJ, Kutscha M, Pool EM, Rehme AK, Eickhoff SB, *et al.* (2014): Dose-dependent effects of theta burst rTMS on cortical excitability and resting-state connectivity of the human motor system. J Neurosci 34:6849–6859.
57. Bestmann S, Baudewig J, Siebner HR, Rothwell JC, Frahm J (2005): BOLD MRI responses to repetitive TMS over human dorsal premotor cortex. NeuroImage 28:22–29.
58. Bestmann S, Swayne O, Blankenburg F, Ruff CC, Haggard P, Weiskopf N, *et al.* (2008): Dorsal premotor cortex exerts state-dependent causal influences on activity in contralateral primary motor and dorsal premotor cortex. Cereb Cortex 18:1281–1291.
59. Mueller S, Wang D, Fox MD, Yeo BTT, Sepulcre J, Sabuncu MR, *et al.* (2013): Individual variability in functional connectivity architecture of the human brain. Neuron 77:586–595.
60. Fox MD, Buckner RL, White MP, Greicius MD, Pascual-Leone A (2012): Efficacy of transcranial magnetic stimulation targets for depression is related to intrinsic functional connectivity with the subgenual cingulate. Biol Psychiatry 72:595–603.
61. Weigand A, Horn A, Caballero R, Cooke D, Stern AP, Taylor SF, *et al.* (2018): Prospective validation that subgenual connectivity predicts antidepressant efficacy of transcranial magnetic stimulation sites. Biol Psychiatry 84:28–37.
62. Cash RFH, Zalesky A, Thomson RH, Tian Y, Cocchi L, Fitzgerald PB (2019): Subgenual functional connectivity predicts antidepressant treatment response to transcranial magnetic stimulation: Independent validation and evaluation of personalization. Biol Psychiatry 86:e5–e7.
63. Stokes MG, Chambers CD, Gould IC, English T, McNaught E, McDonald O, *et al.* (2007): Distance-adjusted motor threshold for transcranial magnetic stimulation. Clin Neurophysiol 118:1617–1625.
64. Caulfield KA, Li X, George MS (2021): Four electric field modeling methods of dosing prefrontal transcranial magnetic stimulation (TMS): Introducing APEX MT dosimetry. Brain Stimul 14:1032–1034.
65. Numssen O, Kuhnke P, Weise K, Hartwigsen G (2024): Electric-field-based dosing for TMS. Imaging Neurosci 2:1–12.
66. Hanlon CA, Canterberry M, Taylor JJ, DeVries W, Li X, Brown TR, *et al.* (2013): Probing the frontostriatal loops involved in executive and limbic processing via interleaved tms and functional MRI at two prefrontal locations: A pilot study. PLoS One 8:e67917.
67. Dowdle LT, Brown TR, George MS, Hanlon CA (2018): Single pulse TMS to the DLPFC, compared to a matched sham control, induces a direct, causal increase in caudate, cingulate, and thalamic BOLD signal. Brain Stimul 11:789–796.
68. Weiskopf N, Josephs O, Ruff CC, Blankenburg F, Featherstone E, Thomas A, *et al.* (2009): Image artifacts in concurrent transcranial magnetic stimulation (TMS) and fMRI caused by leakage currents: Modeling and compensation. J Magn Reson Imaging 29:1211–1217.